Vaccine 37 (2019) 3154–3158

Contents lists available at ScienceDirect

Vaccine

journal homepage: www.elsevier.com/locate/vaccine

Short communication

Modular epitope binding predicts influenza quasispecies dominance and vaccine effectiveness: Application to 2018/19 season

Melia E. Bonomo [a,b], Rachel Y. Kim [c], Michael W. Deem [a,b,d,*]

[a] Department of Physics and Astronomy, Rice University, 6100 Main St, Houston, TX 77005, USA
[b] Center for Theoretical Biological Physics, Rice University, 6100 Main St, Houston, TX 77005, USA
[c] Weiss School of Natural Sciences, Rice University, 6100 Main St, Houston, TX 77005, USA
[d] Department of Bioengineering, Rice University, 6100 Main St, Houston, TX 77005, USA

ARTICLE INFO

Article history:
Received 14 January 2019
Received in revised form 11 March 2019
Accepted 28 March 2019
Available online 3 May 2019

Keywords:
Seasonal influenza
Immunity
Antigenic distance
Mathematical models
Vaccine effectiveness
Vaccination planning

ABSTRACT

The modular binding sites on the influenza A(H3N2) hemagglutinin protein are under significant pressure to acquire mutations in order to evade human antibody recognition. Analysis of these hemagglutinin epitopes in the strains circulating during 2017/18 and early 2018/19 identified the emergence of a new antigenic cluster that has grown from 4% of circulating strains to 11%. We regressed our module-based antigenic distance, p_{epitope}, with A(H3N2) vaccine effectiveness from recent studies conducted by the US Centers for Disease Control and Prevention ($r^2 = 0.92$), and we used this to estimate that the 2018/19 vaccines will protect against most circulating A(H3N2) strains. The pEpitope model is useful for A(H3N2) influenza vaccine virus selection and development, and it has the potential to aid national or regional regulatory authorities in making geographically localized decisions.

1. Introduction

Of the two influenza surface proteins that the human immune system recognizes, i.e., hemagglutinin (HA) and neuraminidase, there is significant pressure on HA to evolve since most antibodies recognize the virus through five epitopes on its globular head [1,2] (Fig. 1A). Epitopes are modules of amino acids to which the antibody receptor binds. In a gradual process referred to as "antigenic drift," there is selection for mutations in the epitopes that allow the influenza virus to evade antibody recognition [1]. The accumulation of mutations leads HA to evolve as quasispecies clusters in ferret-based antigenic distance space [4] and in amino acid sequence space [5]. These viral quasispecies are clusters of variants that have evolved with similar mutations to be sufficiently distant from the vaccine strain such that they are expected to evade antibody recognition [5]. The virus may additionally acquire binding site mutations during the vaccine manufacturing process, e.g., when it is isolated in chicken eggs [6,7]. The human immune system can tolerate small antigenic distances between the influenza vaccine and infecting virus strains, however quasispecies that emerge at larger distances from the vaccine will not be successfully recognized by primed antibodies. Producing an effective vaccine against this rapidly evolving virus necessitates a comprehensive method to characterize the antigenic distance sensitivity in humans.

Previously, we developed a mathematical model that accounts for immunological diversity, modularity, and hierarchy during human antibody recognition of influenza antigens [8]. The order parameter for antibody fitness, defined as the fractional amino acid differences between an infecting antigen α and antibody from vaccine β, was used to establish a pEpitope model of antigenic distance

$$p^{\alpha\beta}_{epitope} = \max_k p^{\alpha\beta}_k = \max_k \frac{n^{\alpha\beta}_k}{N_k} \tag{1}$$

where $n^{\alpha\beta}_k$ is the number of amino acid differences between α and β in epitope k, N_k is the total number of amino acids in epitope k, and k is evaluated for each epitope, *e.g.*, A, B, C, D, and E for A(H3N2). The hierarchy of $p^{\alpha\beta}_k$ distances determines the capability of antibody recognition, as the epitope with the largest $p^{\alpha\beta}$ is considered immunodominant, k^* (Fig. 1B). Prior work demonstrated the pEpitope model's predictability of vaccine efficacy in humans for influenza B [9], A(H1N1) [10], and A(H3N2) [7]. The use of p_{epitope} to predict vaccine effectiveness, which is well-suited to estimate

* Corresponding author at: 6500 Main St STE 1030, Rice University, Houston, TX 77030, USA.
E-mail addresses: meb16@rice.edu (M.E. Bonomo), ryk4@rice.edu (R.Y. Kim), mwdeem@rice.edu (M.W. Deem).

https://doi.org/10.1016/j.vaccine.2019.03.068
0264-410X/

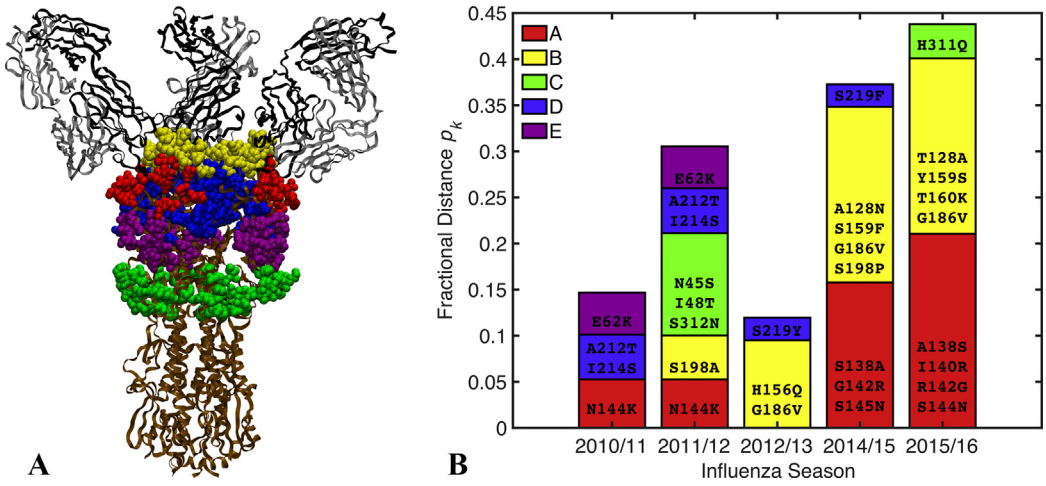

Fig. 1. (A) The HA trimer of A/Victoria/361/2011(H3N2) in complex with three human antibody fragments. The pEpitope model compares the epitope regions A (red; amino acid residues 122, 124, 126, 130–133, 135, 137, 138, 140, 142–146, 150, 152, 168), B (yellow; residues 128, 129, 155–160, 163, 165, 186–190, 192–194, 196–198), C (green; residues 44–48, 50, 51, 53, 54, 273, 275, 276, 278–280, 294, 297, 299, 300, 304, 305, 307–312), D (blue; residues 96, 102, 103, 117, 121, 167, 170–177, 179, 182, 201, 203, 207–209, 212–219, 226–230, 238, 240, 242, 244, 246–248), and E (purple; residues 57, 59, 62, 63, 67, 75, 78, 80–83, 86–88, 91, 92, 94, 109, 260–262, 265) [2] of the dominant circulating strains to those of the vaccine. During the 2012/13 season, A/Victoria/361/2011 was the dominant circulating strain and epitope B was immunodominant. The image was rendered in Visual Molecular Dynamics [3] from Protein Data Bank entry 4O5I. (B) Fractional differences, p_k (Eq. (1)), in the amino acids of each epitope between the vaccine and dominant circulating virus strains during five seasons (Table 1). Individual amino acid mutations are reported in each bar. The largest stacked bar in each season measures p_{epitope}, and that epitope is k^*. (For interpretation of the references to color in this figure legend, the reader is referred to the web version of this article.)

Table 1
Data from the US Centers for Disease Control and Prevention Influenza Vaccine Effectiveness Network. The p_{epitope} distances and immunodominant epitope k^* are determined for each A(H3N2) vaccine and dominant strain pair using Eq. (1). Accession numbers are for the GISAID database [12]. CVV: candidate vaccine virus, VE: vaccine effectiveness (Eq. (2)), CH: Switzerland, HK: Hong Kong.

Season	CVV	Dominant Strain	p_{epitope}	k^*	VE (%)
2010/11	A/Perth/16/2009 (EPI577972)	A/Victoria/208/2009 (EPI272062)	0.053	A	41 ± 12 [14]
2011/12	A/Perth/16/2009 (EPI577972)	A/Victoria/361/2011 (EPI545346)	0.111	C	36 ± 10 [15]
2012/13	A/Victoria/361/2011 (EPI408194)	A/Victoria/361/2011 (EPI545346)	0.095	B	37 ± 6 [16]
2014/15	A/Texas/50/2012 (EPI397876)	A/California/02/2014 (EPI517095)	0.191	B	6 ± 7 [17]
2015/16	A/CH/9715293/2013 (EPI537866)	A/HK/4801/2014 (EPI539576)	0.211	A	−11 ± 33 [18]

vaccine performance from case-control-type studies [11], or detect quasispecies has not been studied before. We used this module-based antigenic distance to determine influenza subtype A(H3N2) quasispecies emergence during the 2018/19 northern hemisphere influenza season and to estimate average vaccine effectiveness and effectiveness against specific A(H3N2) variants.

2. Methods

2.1. Antigenic analysis of circulating A(H3N2) influenza viruses, 2017/18 and 2018/19

We obtained HA sequences from the Global Initiative on Sharing All Influenza Data (GISAID) EpiFlu™ database [12] for all A (H3N2) strains circulating between September 2017 and December 2018. After removing passaged and incomplete strains, we utilized 374 strains collected in September 2017, 560 in October, 700 in November 1001 in December 1064 strains collected in January 2018, 549 in February, 381 in March, 141 in April, and 31 in May, for a total of 4801 strains in the 2017/18 season. For the early 2018/19 season, we utilized 83 strains collected in June 2018, 56 in July, 42 in August, 49 in September, 49 in October, 50 in November, and 8 strains in December, for a total of 337 strains. We additionally obtained HA sequences for the two candidate vaccine viruses (CVV) that the World Health Organization (WHO) recommended for the 2018/19 northern hemisphere season, egg-based A/Singapore/INFIMH-16-0019/2016 and cell-based A/North Carolina/04/2016.

The antigenic distance was calculated between all pairs of strains by determining the number of amino acid differences in each epitope, and taking the maximum p_k to be p_{epitope} (Eq. (1)). We created a pEpitope Calculator application for MATLAB that can be downloaded [13]. Multidimensional scaling was performed using the MATLAB Statistics and Machine Learning Toolbox™, and the p_{epitope}-distance spaces for 2017/18 and 2018/19 were each reduced to two dimensions.

2.2. Calibration of pEpitope model for predicting vaccine effectiveness

Our primary vaccine effectiveness dataset (Table 1) was compiled by the US Centers for Disease Control and Prevention (CDC) from studies conducted in their Influenza Vaccine Effectiveness Network (US Flu VE Network). These data were from test-negative design case-control studies that confirmed A(H3N2)-positive from real-time reverse-transcriptase polymerase chain reaction (RT-PCR) and included a representative sample of the US population and of vaccine coverage. A separate 47-year dataset (Supplementary Table 1) was obtained from individually-published studies in the northern hemisphere from the 1971/72 season through the 2017/18 season. We isolated a subset of these data from the past decade, *i.e.*, 2008/09 to 2017/18, to represent a third dataset. For each study, we obtained the total number of vaccinated individuals, the total number of unvaccinated individuals, and the number of vaccinated and unvaccinated cases, *i.e.*, individuals who tested positive for A(H3N2) in the study. We focused on individuals between the ages of 18–65 in order to avoid

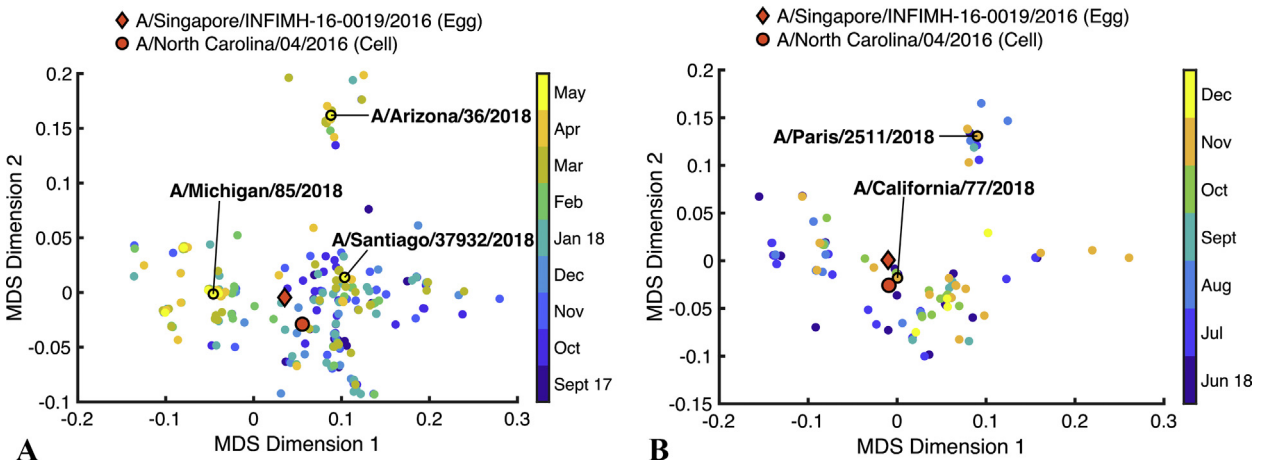

Fig. 2. Multidimensional scaling (MDS) of $p_{epitope}$-distance space for the 2018/19 egg- and cell-based vaccines and all circulating A(H3N2) strains during the (A) 2017/18 and (B) early 2018/19 seasons. The color-bar denotes the month of strain collection. A/Michigan/85/2018 was homologous and A/California/77/2018 was nearly-homologous in the epitope regions to the consensus sequences in each MDS plot. Due to their distances from the main cluster and their increasing percentage from 2017/18 to early 2018/19, A/Arizona/36/2018-like and A/Paris/2511/2018-like variants are identified as an emerging quasispecies. The $p_{epitope}$ distances are summarized in Supplementary Table 2.

confounding effects related to developing immune systems in children or to immunosenescence in older adults. Vaccine effectiveness [11] was calculated as

$$\text{Vaccine Effectiveness} = 1 - \frac{OV}{OU} \quad (2)$$

where the odds in the vaccinated group, OV, and the odds in the unvaccinated group, OU, are

$$OV = \frac{\text{vaccinated A(H3N2) cases}}{\text{vaccinated controls}} \text{ and}$$
$$OU = \frac{\text{unvaccinated A(H3N2) cases}}{\text{unvaccinated controls}} \quad (3)$$

We downloaded the HA sequence for the "antigenically like" A (H3N2) strain recommended to be included in influenza vaccines and the dominant circulating strain published by the WHO each season [19]. The HA binding sites in each CVV were compared to those in the dominant infecting strain for each season, and Eq. (1) was again used to calculate antigenic distance. Linear regression was performed using linear least squares fitting with the vaccine effectiveness data and $p_{epitope}$ values. No data were excluded from analysis.

3. Results

3.1. Emergence of an A(H3N2) quasispecies during the 2018/19 season

Multidimensional scaling of the 2017/18 circulating strains revealed one large cluster, with two centroids, near the WHO-recommended 2018/19 CVVs and a smaller, comparatively distant cluster (Fig. 2A). The A/Arizona/36/2018 strain representative of the distant cluster had a $p_{epitope}$ of 0.191 from both of the CVV strains, approximately where vaccine effectiveness has gone to zero in the past [5]. The A/Arizona/36/2018 cluster contained 174 strains, or 3.6% of all those circulating in 2017/18. Multidimensional scaling of the early 2018/19 strains again revealed a broad cluster and a smaller, relatively distant one (Fig. 2B). The A/Paris/2511/2018 strain representative of this distant cluster is homologous to A/Arizona/36/2018 in the epitope regions. This A/Paris/2511/2018 cluster contains 36 strains, or 10.7% of those circulating in early 2018/19. Multidimensional scaling of the A/Arizona/36/2018 and A/Paris/2511/2018 clusters reveals that these variants are part of the same viral quasispecies (Supplementary Fig. 1).

3.2. Prediction of effectiveness for the 2018/19 A(H3N2) vaccines

We assessed the relation between the observed vaccine effectiveness in the three datasets and the pEpitope model (Fig. 3). Linear regression between the $p_{epitope}$ distances and the observed vaccine effectiveness from the US Flu VE Network studies produced

$$\text{Vaccine Effectiveness} = (-3.32p_{epitope} + 0.66) \times 100\% \quad (4)$$

with a coefficient of determination (r^2) of 0.92 (slope p-value = 0.0095, intercept p-value = 0.0039) (Supplementary Table 3). Analyzing all the epidemiological data in the northern hemisphere from the past 47 years, the pEpitope model yielded an r^2 of 0.75. Limiting the analysis to recent data from seasons 2008/09 to 2017/18, the pEpitope model yielded an r^2 of 0.78. See Supplementary

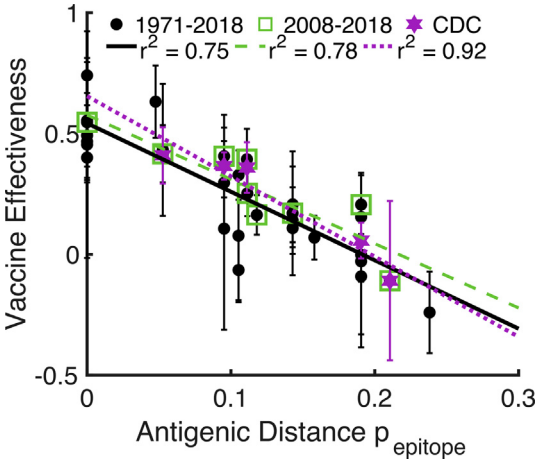

Fig. 3. The pEpitope model calibrated with human vaccine effectiveness data. The vertical axes show vaccine effectiveness from 1971/72 to 2017/18 (black circle markers, solid line), 2008/09 to 2017/18 (green square markers, dashed line), and test-negative design studies in the CDC's US Flu VE Network from 2010/11 to 2015/16 (purple star markers, dotted line). Vaccine effectiveness was computed for each season by Eq. (2). Lines represent linear regressions and r^2 are coefficients of determination (Supplementary Table 3). (For interpretation of the references to color in this figure legend, the reader is referred to the web version of this article.)

Material for a comparison of the pEpitope vaccine effectiveness model with ferret-based antigenic distances and with vaccine efficacy.

On average against all circulating strains during the 2017/18 season, the egg-based CVV has a 0.121 $p_{epitope}$ distance, and Eq. (4) predicts the vaccine effectiveness to be 25 ± 11%. The cell-based CVV, with a 0.111 $p_{epitope}$ distance, is predicted to be 29 ± 10% effective. Based on the higher average $p_{epitope}$ distances against strains circulating during the early 2018/19 season, the predicted effectiveness has gone down to 21 ± 11% for the egg-based CVV and 25 ± 11% for the cell-based CVV. The average effectiveness is predicted to be low because Eq. (4) estimates that both CVVs are 2 ± 13% effective against the A/Arizona/36/2018 and A/Paris/2511/2018 clusters. However, the 2018/19 vaccines are anticipated to perform better against the majority of 2018/19 A (H3N2) strains, which are A/California/77/2018-like, at 34 ± 10% and 31 ± 10% for the egg and cell CVVs, respectively.

4. Discussion

The pEpitope model was readily able to estimate the antigenic distance either between individual CVV and dominant circulating strain pairs, or between thousands of influenza strains. Analysis of all circulating strains in $p_{epitope}$-distance space predicted that both the egg- and cell-based CVVs will have positive effectiveness against the majority of strains during the 2018/19 season. The analysis also suggested a small cluster of strains that are antigenically-like A/Arizona/36/2018 is emerging at a $p_{epitope} > 0.19$ from the current CVVs, beyond the limit for effective immune protection. This is in agreement with the distance at which we have seen new antigenic quasispecies evolving in clusters historically [5]. There is likely to be increased selection for A/Arizona/36/2018-like strains if the A(H3N2) vaccine component remains at a $p_{epitope}$ distance > 0.19, given the lack of protection against strains that are this distant.

These predictions are based on the pEpitope model being able to explain much of the variance in vaccine effectiveness data from humans in recent studies conducted by the US Flu VE Network, over the past 47 years, and over the past decade. The vaccine manufacture and administration protocols as well as the diagnosis methodologies of influenza versus influenza-like illness during clinical studies have strengthened over time [6]. Therefore, epidemiological data from the past decade were expected to benefit from these improvements in the field, and the pEpitope model demonstrated a greater coefficient of determination over the past decade as compared to over the past 47 years. The $r^2 = 0.92$ on the US Flu VE Network dataset suggested the pEpitope model has heightened predictability when it is calibrated using studies that are geographically localized and have high consistency in data collection and clinical procedures.

Several recent studies have identified specific amino acid substitutions that have been key to many past substantial antigenic changes [1]. However, we believe the comprehensive approach presented here that considers all of the antigenic sites is important to detect future antigenic drift and substantial antigenic changes during the manufacturing process. For instance, low vaccine effectiveness during the 2016/17 season was suggested to have resulted from an egg-adapted substitution at site 160 in epitope B, which was identified both by biochemical analysis [20] and by the pEpitope model [7], but was not previously identified as a key substitution site.

5. Limitations

There is a complexity of factors that may influence antibody recognition of influenza HA antigens. For one, there is evidence to suggest that prior influenza vaccinations have differential effects on the antigenic distance seen by the human immune system to new infections [21]. Additionally, structural studies of the influenza HA glycosylation state have shown that glycans can shield the surrounding amino acids [22], thereby potentially inhibiting antibody recognition further than do individual amino acid mismatches. Additional work is needed to assess the potential benefits of incorporating these factors into the $p_{epitope}$ measure of antigenic distance.

Our present study focuses on the effectiveness of the A(H3N2) vaccine component and therefore cannot estimate the overall performance of the 2018/19 vaccine. Interim estimates from test-negative design case-control studies conducted by the CDC US Flu VE Network have shown that A(H1N1) has been the predominant subtype during the 2018/19 season [23]. Future work will incorporate analyses of the A(H1N1), B/Yamagata/16/88 lineage, and B/Victoria/2/87 lineage vaccine components to produce a complete model of influenza vaccine effectiveness.

6. Conclusions

These results suggest that the pEpitope model is useful to several aspects of virological characterization for design and manufacture of the A(H3N2) vaccine component. This module-based antigenic distance aids in the selection of specimen strains for the vaccine that are predicted to effectively prime human antibodies against the majority of circulating strains. While there are existing forecasting models for the dominant seasonal strains [6] and the emergence of quasispecies from antigenic drift in animal models [4], pEpitope adds an additional dimension to increase the likelihood that the chosen specimen minimizes antigenic distance within the dominant cluster to which the human immune system is sensitive.

The pEpitope model can check that the viruses that have been isolated and reassorted with high growth properties by vaccine producers continue to maintain their key antigenic features. There have been several seasons in which the specimen selected for the vaccine was well-chosen to match dominant circulating strains, however the egg-isolated CVV contained critical antigenic changes that ultimately lowered vaccine efficacy [7]. The pEpitope model successfully identified these changes.

Finally, the pEpitope model contributes to health policy and vaccine planning regarding localized geographical vaccination choices. The national or regional regulatory authorities and control laboratories that determine the vaccine composition for each country could utilize the pEpitope model when choosing from the WHO's list of CVVs. There are slight antigenic differences between these CVVs that may match up to strains dominating in particular geographical regions. Several vaccine choices can be rapidly analyzed against thousands of strains circulating in a particular region to help make these localized decisions.

Note added in proof

While this paper was in review, the CDC released an addendum to the recommended composition of influenza virus vaccines for use in the 2019/20 northern hemisphere influenza season (https://www.who.int/influenza/vaccines/virus/recommendations/201902_recommendation_addendum.pdf), announcing an A/Kansas/14/2017-like virus as the A(H3N2) component. This A/Kansas/14/2017 specimen (EPI1146345) is identical in the HA region to A/Arizona/36/2018 (EPI1256668), which was the representative strain of the emerging quasispecies identified by our pEpitope model.

Funding

This work was supported by the Center for Theoretical Biological Physics at Rice University, Houston TX [National Science Foundation, PHY 1427654] and the Welch Foundation [C-1917-20170325].

Author contributions

MWD conceived the project and provided guidance. MEB and RYK analyzed data. MEB, RYK, and MWD interpreted data. MEB and MWD designed the pEpitope Calculator app. MEB and RYK developed the first draft of the manuscript. MEB and MWD revised and edited the manuscript. MEB designed figures. All authors approved the final manuscript.

Acknowledgements

We would like to thank Jacqueline M. Katz, Alicia M. Fry, and Ivo M. Foppa at the CDC for helpful discussions regarding the datasets and methods of this paper.

Conflict of interest

None.

Appendix A. Supplementary material

Supplementary data to this article can be found online at https://doi.org/10.1016/j.vaccine.2019.03.068.

References

[1] Petrova VN, Russell CA. The evolution of seasonal influenza viruses. Nat Rev Microbiol 2018;16(1):47.
[2] Munoz ET, Deem MW. Epitope analysis for influenza vaccine design. Vaccine 2005;23(9):1144–8.
[3] Humphrey W, Dalke A, Schulten K. VMD: visual molecular dynamics. J Mol Graph 1996;14(1):33–8.
[4] Smith DJ, Lapedes AS, de Jong JC, Bestebroer TM, Rimmelzwaan GF, Osterhaus AD, et al. Mapping the antigenic and genetic evolution of influenza virus. Science 2004;305(5682):371–6.
[5] He J, Deem MW. Low-dimensional clustering detects incipient dominant influenza strain clusters. Protein Eng Des Sel 2010;23(12):935–46.
[6] Hampson A, Barr I, Cox N, Donis RO, Siddhivinayak H, Jernigan D, et al. Improving the selection and development of influenza vaccine viruses–Report of a WHO informal consultation on improving influenza vaccine virus selection, Hong Kong SAR, China, 18–20 November 2015. Vaccine 2017;35(8):1104–9.
[7] Bonomo ME, Deem MW. Predicting influenza H3N2 vaccine efficacy from evolution of the dominant epitope. Clin Infect Dis 2018;67(7):1129–31.
[8] Sun J, Earl DJ, Deem MW. Localization and glassy dynamics in the immune system. Mod Phys Lett B 2006;20(02n03):63–95.
[9] Pan Y, Deem MW. Prediction of influenza B vaccine effectiveness from sequence data. Vaccine 2016;34(38):4610–7.
[10] Pan K, Subieta KC, Deem MW. A novel sequence-based antigenic distance measure for H1N1, with application to vaccine effectiveness and the selection of vaccine strains. Protein Eng Des Sel 2010;24(3):291–9.
[11] Weinberg GA, Szilagyi PG. Vaccine epidemiology: efficacy, effectiveness, and the translational research roadmap. J Infect Dis 2010;201(11):1607–10.
[12] Shu Y, McCauley J. GISAID: Global initiative on sharing all influenza data – from vision to reality. EuroSurveillance 2017;22(13).
[13] http://www.mwdeem.rice.edu/pepitope/.
[14] Treanor JJ, Talbot HK, Ohmit SE, Coleman LA, Thompson MG, Cheng P, et al. Effectiveness of seasonal influenza vaccines in the United States during a season with circulation of all three vaccine strains. Clin Infect Dis 2012;55(7):951–9.
[15] Ohmit SE, Thompson MG, Petrie JG, Thaker SN, Jackson ML, Belongia EA, et al. Influenza vaccine effectiveness in the 2011–2012 season: protection against each circulating virus and the effect of prior vaccination on estimates. Clin Infect Dis 2013;58(3):319–27.
[16] McLean HQ, Thompson MG, Sundaram ME, Kieke BA, Gaglani M, Murthy K, et al. Influenza vaccine effectiveness in the United States during 2012–2013: variable protection by age and virus type. J Infect Dis 2014;211(10):1529–40.
[17] Zimmerman RK, Nowalk MP, Chung J, Jackson ML, Jackson LA, Petrie JG, et al. 2014–2015 influenza vaccine effectiveness in the United States by vaccine type. Clin Infect Dis 2016;63(12):1564.
[18] Jackson ML, Chung JR, Jackson LA, Phillips CH, Benoit J, Monto AS, et al. Influenza vaccine effectiveness in the United States during the 2015–2016 season. N Engl J Med 2017;377(6):534–43.
[19] http://www.who.int/influenza/vaccines/virus/recommendations/.
[20] Zost SJ, Parkhouse K, Gumina ME, Kim K, Perez SD, Wilson PC, et al. Contemporary H3N2 influenza viruses have a glycosylation site that alters binding of antibodies elicited by egg-adapted vaccine strains. PNAS USA 2017;114(47):12578–83.
[21] Xie H, Li L, Ye Z, Li X, Plant EP, Zoueva O, et al. Differential effects of prior influenza exposures on H3N2 cross-reactivity of human postvaccination sera. Clin Infect Dis 2017;65(2):259–67.
[22] Kobayashi Y, Suzuki Y. Evidence for N-glycan shielding of antigenic sites during evolution of human influenza A virus hemagglutinin. J Virol 2012; p. JVI–06147.
[23] Doyle JD, Chung JR, Kim SS, Gaglani M, Raiyani C, Zimmerman RK, et al. Interim estimates of 2018–19 seasonal influenza vaccine effectiveness—United States, February 2019. MMWR Morb Mortal Wkly Rep 2019;68:135–9.